applied sciences

MDPI

Article

Experimental Study on Confined Compaction Deformation of Crushed Gangue under Different Water Content Conditions

Pengfei Liang [1,*], Yu Yang [1], Jiashun Liu [1], Changhao Xin [1] and Yidan Sun [2]

[1] College of Civil Engineering, Liaoning Technical University, Fuxin 123000, China; yangyu9300@163.com (Y.Y.); liujiashun000@163.com (J.L.); 472120637@stu.lntu.edu.cn (C.X.)
[2] College of Civil and Marine Engineering, Jiangsu Ocean University, Lianyungang 222000, China; 2020000083@jou.edu.cn
* Correspondence: 472010038@stu.lntu.edu.cn; Tel.: +86-138-4181-5998

Abstract: To study the deformation characteristics of crushed gangue under different water content conditions, the confined compaction test of crushed gangue was carried out under five different water content conditions by using a universal material testing machine and a compaction device. The strain–stress relationship in the compaction process of crushed gangue and the crushing law of gangue particles were obtained through the test, and the effects of the axial stress, water content, and relative crushing rate on the compaction deformation of crushed gangue were analyzed. The results show that the confined compaction deformation process of crushed gangue can be divided into three stages: the rapid compaction stage, crushing compaction stage, and stable compaction stage. The strain–stress relationship can be described by the parameter logarithmic function and Chapman–Richards function, respectively. The maximum change in the compression modulus under different water content states ranged from 9.9 to 19.3 MPa, and the influence of the water content on the compression modulus was more significant with increasing axial stress. There is a good correlation between particle crushing and compaction deformation. The relative crushing rate increases with the increase in the axial strain, and the increasing rate of the relative crushing rate also gradually increases. The change law of the relative crushing rate and axial strain is different in dry and water-containing conditions.

Keywords: crushed gangue; confined compaction; deformation law; particle crushing; relative crushing rate

check for updates

Citation: Liang, P.; Yang, Y.; Liu, J.; Xin, C.; Sun, Y. Experimental Study on Confined Compaction Deformation of Crushed Gangue under Different Water Content Conditions. *Appl. Sci.* **2023**, *13*, 4538. https://doi.org/10.3390/app13074538

Academic Editor: Muhammad Junaid Munir

Received: 16 March 2023
Revised: 1 April 2023
Accepted: 2 April 2023
Published: 3 April 2023

Copyright: © 2023 by the authors. Licensee MDPI, Basel, Switzerland. This article is an open access article distributed under the terms and conditions of the Creative Commons Attribution (CC BY) license (https://creativecommons.org/licenses/by/4.0/).

1. Introduction

Coal gangue is the solid waste generated during the mining and washing of coal resources, accounting for about 10% to 30% of coal production [1,2]. For a long time, the overall utilization efficiency of coal gangue has been low, and a large amount of coal gangue needs to be stored in open-air piles, which has led to increasingly prominent ecological and environmental problems [3–6]. The accumulation of coal gangue not only occupies a large amount of land resources but also causes geological disasters, such as landslides and debris flows. Under the effects of the leaching and infiltration of rainwater, coal gangue can produce toxic elements that pollute soil and groundwater resources [7]. Toxic and harmful gases such as sulfur dioxide produced during the spontaneous combustion of coal gangue also cause pollution to the atmospheric environment. The ecological restoration, development, and utilization of the historical accumulated gangue hills are relatively complex and difficult, involving interdisciplinary applications of geology, hydrology, the atmosphere, the environment, and other fields [8,9]. In recent years, although China has continuously increased its investment in the restoration, management, and development and utilization of historical accumulated gangue hills, it still faces many problems and challenges [10–12].

Coal gangue has become an important geotechnical filling material for the comprehensive utilization of coal gangue. In addition to filling coal mining and backfilling subsidence areas, it is also widely used in civil engineering for applications, such as road embankment filling, hydraulic engineering dam construction, and construction engineering foundation cushioning [13–18]. According to the classification of civil engineering materials, coal gangue belongs to coarse-grained soil, and its compaction characteristics are important for ensuring its effectiveness in engineering applications. The physical and mechanical properties of coal gangue vary greatly in different compaction states. To better apply coal gangue in engineering, many scholars have conducted extensive research on the pressure characteristics of coal gangue through laboratory tests since the end of the last century. Ma [19] and Huang [20] summarized the correlation between the stress and strain, porosity, and deformation modulus during the compaction process of coal gangue through compaction tests on both loose and saturated gangue, and they analyzed the influence of the gangue particle size and saturation state on its compaction characteristics. Jiang [21] and Wang [22] studied the relationship between the coal gangue particle size distribution and compaction properties through compaction tests. The low content of fine particles is the main defect of natural coal gangue gradation. A large proportion of soft rock gangue is crushed during the compaction process, which improves the particle defect of coal gangue and thus improves its compaction degree. Liu et al. [23–25] conducted experimental research on the basic particle size characteristics of coal gangue and pointed out that particle crushing can promote the rearrangement of particles, reduce porosity, and make the compacted structure more compact. However, excessive compaction can continuously refine gangue particles, thereby weakening the occlusal effect between coarse particles. Zheng [26] discovered that both the Weibull distribution and fractal distribution can represent the distribution law of the coal gangue crushing particle size, and the expression effect of the fractal distribution is better. To study the fractal characteristics of compacted coal gangue, Zhang [27] performed compaction tests under different stresses and particle sizes. The results showed that the particle size distribution of coal gangue samples exhibited fractal characteristics, and the fractal dimension increased with the increase in the small particle content, and tended to a certain value. Rujikiatkamjorn [28] analyzed the geotechnical properties of coal gangue through experiments. Compared to sandy fillers, coal gangue has a relatively low maximum dry density. If it is compacted properly, it shows potential as a good reclamation material, which can help reduce the long-term settlement of the underlying clay layer. Yang [29] discovered that under the same stress conditions, the smaller the particle size of gangue and the smaller the loading rate, the smaller the compaction deformation and the more energy consumed to achieve the same strain. Wang [30] carried out the compaction creep test on a gangue filling body and established the relationship between the axial strain and porosity with time, as well as the influence of the particle size distribution on the relationship. He also developed a consolidation-creep equation for coal gangue that satisfies the Talbot grading distribution. Li [31] proposed a new hybrid artificial intelligence model that combines the support vector machine, differential evolution algorithm, and grey wolf optimization algorithm to predict the compaction characteristics of coal gangue filling materials. Zhang [32] obtained the particle gradation change law of the coal gangue subgrade before and after the cyclic dynamic load test through experiments and established a particle crushing evolution model. Li [33] studied the layered crushing characteristics of crushed gangue by using the acoustic emission three-dimensional positioning method. Zhang [34] studied the changing law of the re-crushing of gangue particles under the combined influence of axial stress and particle size distribution, and they analyzed the particle size distribution and fractal characteristics of the re-crushing particles. These research results mainly focus on the basic compaction characteristics of coal gangue, the regularity of particle distribution, and the influencing factors of compaction deformation. However, there has been little research on the influence of the water content in coal gangue on compaction characteristics, as well as on the changes in particle size distribution fractal features before and after compaction.

This study conducted confined compaction tests on crushed gangue under different water conditions, analyzed the compaction deformation characteristics of the gangue samples and the particle crushing characteristics before and after compaction, and obtained the influence law of the water content in crushed gangue on the axial strain and the changing rule between particle crushing and compaction deformation. The research results can provide a useful reference for the determination of the construction technology determination and compaction effect evaluation of coal gangue as roadbed filling material, while also providing a way to ensure the stability of the roadbed when constructing high-grade roads on gangue hills, which is of great significance to alleviate the pressure of a building materials shortage and reduce the ecological environment problems caused by the accumulation of coal gangue.

2. Experiment

2.1. Instrument

Figure 1 shows the electro-hydraulic servo universal material testing machine (WES-1000B, Wuxi Huaxi Building Material Testing Instrument Co., Ltd., Wuxi, China) that was used for the confined compaction test on crushed gangue. The instrument is capable of providing a maximum load of 1000 kN, and the entire experiment process can automatically measure and collect data, such as load and displacement. The compacting device consists of a loading pressure head, steel cylinder, and base. The steel cylinder is made of seamless steel pipe, with a wall thickness of 13 mm, an inner diameter of 150 mm, and a height of 230 mm. The samples were sieved before and after compaction, using a new standard soil sieve (0.075–60 mm, Shaoxing Highway Instrument Equipment Co., Ltd., Shaoxing, China).



Figure 1. Electro-hydraulic servo universal material testing machine and compacting device.

2.2. Experimental Sample

2.2.1. Basic Physical Properties

The study chose the washed coal gangue from the Fuxin area gangue hill as the research object. The gangue is gray-black in color, mainly composed of particles with a large difference in particle size. Table 1 shows the test results of the basic physical properties of the crushed gangue before the test.

Table 1. Basic physical parameters of crushed gangue.

Natural Bulk Density /kg·m^{-3}	Tapped Bulk Density /kg·m^{-3}	Apparent Density /kg·m^{-3}	Surface Dry Density /kg·m^{-3}	Gross Volume Density /kg·m^{-3}	Water Absorption/%
1295	1551	2520	2369	2269	4.50

2.2.2. Determination of Initial Gradation

In order to simulate the original gradation state of the crushed gangue as closely as possible, samples were taken at 10 sampling points and screening tests were carried out. The average gradation of the 10 samples was used as the initial gradation of the crushed gangue for the confined compaction test. Figure 2 shows the average gradation curve of 10 crushed gangue samples.

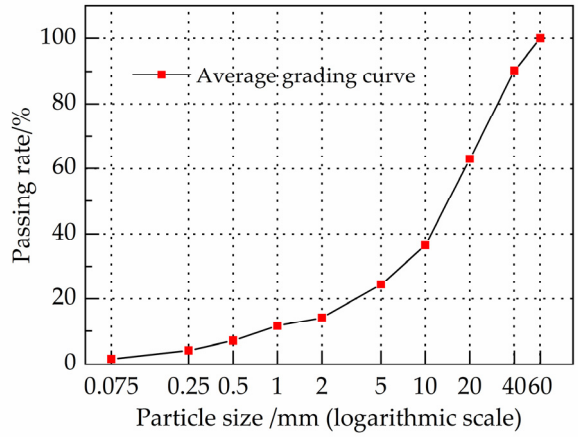


Figure 2. The average gradation curve of 10 crushed gangue samples.

2.2.3. Sample Preparation

According to the size of the steel cylinder, the total mass of samples used for confined compaction test is set to 3800 g per part, from which the mass required for particles of each size can be calculated based on the gradation curve in Figure 2. To prepare the crushed gangue samples with the gradation shown in Figure 2, first the crushed gangue was sieved into 10 particle size intervals by using the new standard soil sieve according to the particle size shown on the horizontal axis of Figure 2. Then, the particles in each particle size interval were blended according to the proportion they occupy. According to the above method, a total of 30 samples with the same gradation were prepared for the confined compaction test. The blended crushed gangue sample is shown in Figure 3.



Figure 3. Crushed gangue sample for confined compaction test.

2.3. Experimental Schemes

To study the effect of different water content conditions on the confined compaction deformation and particle crushing of crushed gangue, as well as the changes in related mechanical properties such as strain–stress, five groups of experiments were designed in this paper. The water content of each group of samples (the percentage of the mass of water in the sample to the mass of dry sample) was set to 0%, 1.5%, 3%, 4.5%, and 6%, respectively [35]. To accurately measure the axial displacement of the crushed gangue samples before and after unloading under different stresses, 6 samples were prepared for each group of experiments for confined compaction tests, and the axial stresses applied to each sample were 4 MPa, 8 MPa, 12 MPa, 16 MPa, 20 MPa, and 24 MPa, respectively. The specific experimental scheme is shown in Table 2.

Table 2. Confined compaction experimental scheme of crushed gangue under different water content conditions.

Test No.	Water Content/%	Axial Stress/MPa
Group 1	0	4, 8, 12, 16, 20, 24
Group 2	1.5	4, 8, 12, 16, 20, 24
Group 3	3.0	4, 8, 12, 16, 20, 24
Group 4	4.5	4, 8, 12, 16, 20, 24
Group 5	6.0	4, 8, 12, 16, 20, 24

According to the experimental scheme set above, prepare test samples with the specified water content, and fill them all into the steel cylinder. Place a steel bar with a diameter of 25mm at the bottom of the cylinder, hold the steel cylinder, and hit the ground alternately 25 times on both sides. Measure the filling height after vibration, install the compaction device on the testing machine for compaction test, and the testing machine loads at a constant rate of 0.5 kN/s. When the applied axial stress reaches the target value, record the axial displacement of the testing machine throughout the compaction process, and measure the compacted height of the sample after unloading the testing machine. Air-dry the crushed gangue sample after compaction and carry out sieving test after drying. Figure 4 shows the detailed test workflow of the testing process.

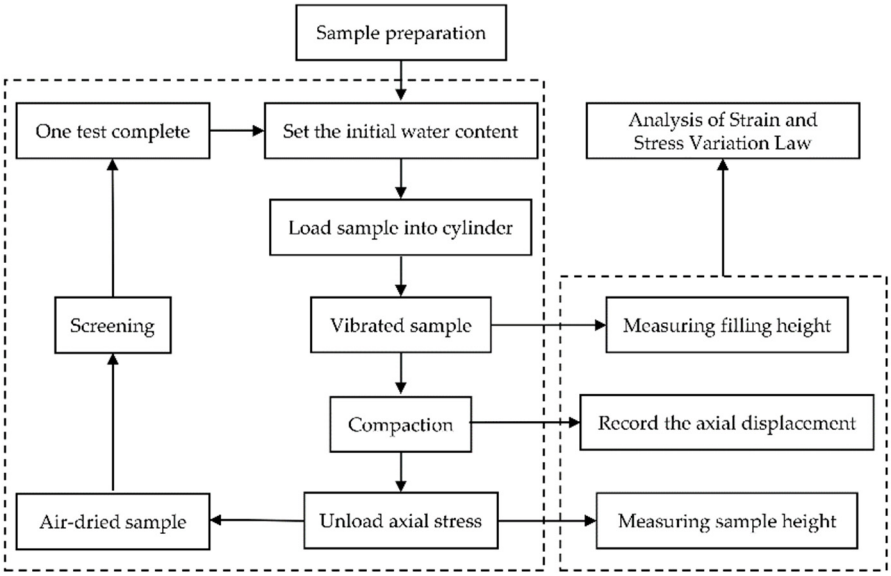


Figure 4. Workflow for confined compaction test of crushed gangue.

3. Results and Analysis

3.1. Analysis of the Strain–Stress Relationship of Confined Compaction

3.1.1. Variation Law of Strain–Stress Curve

The experimental condition for this test is confined compaction, and the compaction device is made of rigid material. The lateral strain is assumed to be zero, and only axial strain occurs during the compaction process. Therefore, the axial strain can be represented as

$$\varepsilon = \frac{\Delta h}{h} \tag{1}$$

where ε is the axial strain, h is the filling height of the sample after vibration, and Δh is the axial displacement during the entire compaction process.

Figure 5 shows the strain–stress curves of the crushed gangue samples compacted from 0 to 24 MPa under 5 different water content conditions. It can be seen from Figure 5 that with the increasing of the axial stress, the axial strain of the samples under different water content conditions generally shows a continuous increasing trend, and the curve increase rate gradually decreases. According to the characteristics of the axial strain–stress curve, the entire confined compaction deformation process of crushed gangue can be divided into three stages: the rapid compaction stage, crushing compaction stage, and stable compaction stage [36,37].

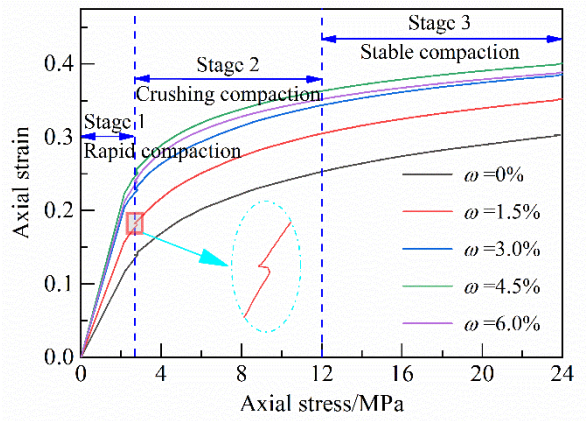


Figure 5. Strain–stress curves of crushed gangue under different water content conditions.

(1) Rapid compaction stage (0–2.8 MPa): At the beginning of loading, the crushed gangue is in a relatively loose state of vibration. As the stress increases, the gangue particles adjust their contact state and continuously fill the pores between the particles. The particles gradually interlock with each other to form a relatively compact skeleton structure, and the crushed gangue samples undergo a relatively large strain under a smaller stress.
(2) Crushing compaction stage (2.8–12 MPa): After the rapid compaction stage, the strain–stress curve has a serrated shape, with a continuous increase in the strain and a small fluctuation in the stress. This is the obvious boundary between the crushing compaction stage and the rapid compaction stage. After the gangue particles are gradually compacted, the stress acting on the skeleton particles that play a supporting role exceeds their strength value, causing the skeleton particles to be concentratedly destroyed. The crushed particles fill the remaining pores, and the stress quickly readjusts, resulting in fluctuations. As the stress continues to increase, the gangue particles continue to slide and roll under the mutual squeezing action, and the gangue particles are crushed again, thus continuously filling the remaining pores.
(3) Stable compaction stage (12–24 MPa): When the compacted state of the crushed gangue reaches a certain degree, the structure of the gangue particles becomes stable, and the residual pores are very small. Under the larger axial stress, the increase in the axial strain is very small. The relationship between the axial strain and axial stress is basically linear, and the axial strain gradually tends to a constant value.

3.1.2. Strain–Stress Curve-Fitting Analysis

The strain–stress curve-fitting equation can well describe the deformation law of crushed gangue under confined compaction. The commonly used fitting forms are the multi-parameter exponential function and logarithmic function, as shown in Equations (2) and (3).

$$\sigma = a \cdot e^{b\varepsilon} \tag{2}$$

$$\varepsilon = a - b\ln(\sigma + c) \tag{3}$$

Although the above two fitting forms have a high degree of fitting with the experimental data, they still have certain shortcomings. Firstly, according to the functional form of the two equations, when the strain value is 0, the stress value calculated by the fitting equation is not 0. Secondly, when the stress increases infinitely, the strain value will also increase infinitely, which is obviously not consistent with the actual situation.

Therefore, in order to better describe the strain–stress laws of the three stages of the confined compaction of crushed gangue, different function forms are adopted to numerically fit the strain–stress curves according to the characteristics of the strain–stress curves in each stage.

The multi-parameter logarithmic function is used for fitting in the rapid compaction stage and the crushing compaction stage, and the Chapman–Richards function is used for fitting in the stable compaction stage. The specific fitting form is shown in Equation (4).

$$\begin{cases} \varepsilon_1 = a_1\ln(b_1\sigma + 1) & \text{Rapid compaction stape} \\ \varepsilon_2 = a_2 - b_2\ln(\sigma + c_2) & \text{Crushing compaction stape} \\ \varepsilon_3 = a_3\left(1 - e^{-b_3\sigma}\right)^{c_3} & \text{Stable compaction stape} \end{cases} \tag{4}$$

where a_1, b_1, a_2, b_2, c_2, a_3, b_3, c_3 are the fitting parameters.

The strain–stress fitting curves under different water content conditions are shown in Figure 6. It can be seen that the piecewise function form of Equation (4) can well express the strain–stress relationship of the crushed gangue under different water content conditions, with the R-squared values all above 0.99. There is a high correlation between the fitting equation and the experimental data.

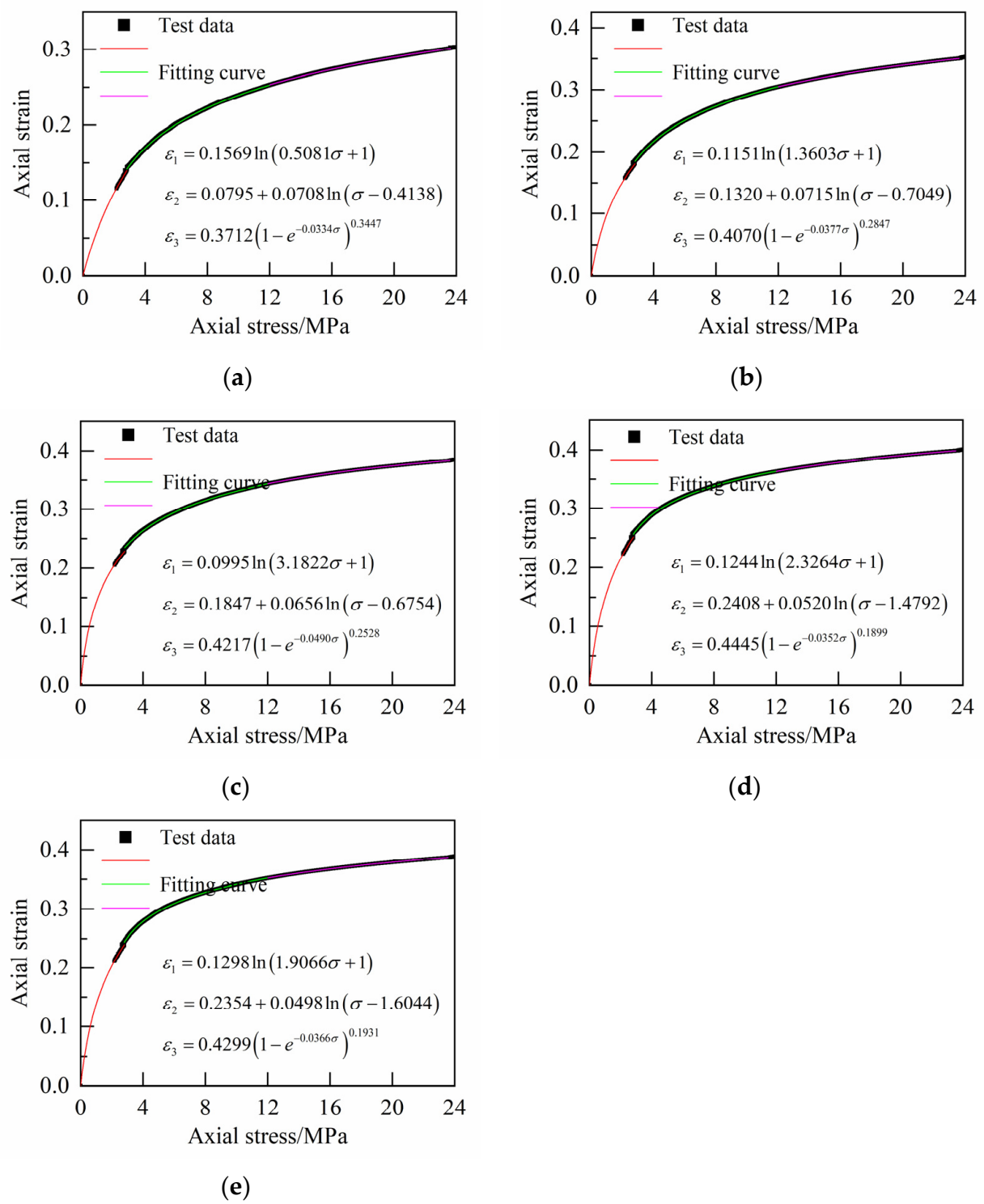


Figure 6. Strain–stress fitting curves under different water content conditions. (**a**) ω = 0%; (**b**) ω = 1.5%; (**c**) ω = 3.0%; (**d**) ω = 4.5%; (**e**) ω = 6.0%.

3.2. Analysis of the Relationship between Compaction Deformation and Water Content

Water content is an important factor affecting the compaction effect of crushed gangue. In order to compare and analyze the influence of the water content on the compaction characteristics, Figure 7 shows the relationship of the axial strain and water content of crushed gangue under different stresses.

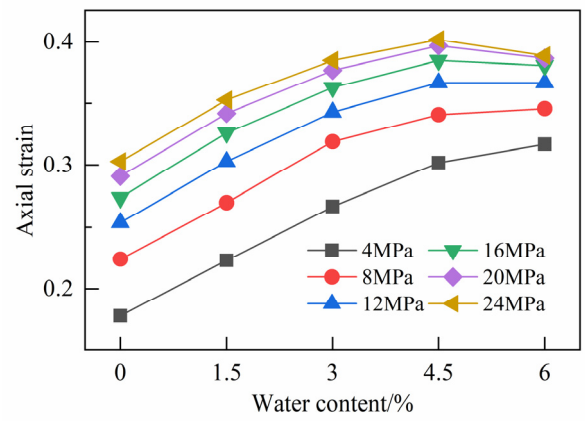


Figure 7. Relationship curves between axial strain and water content.

An analysis based on Figure 7 shows that water content is an important factor affecting the compaction state of crushed gangue. When the maximum axial stress is 4 MPa and 8 MPa, the higher the water content of the crushed gangue, and the greater its axial strain. When the maximum axial stress is 12 MPa, the axial strain first increases continuously with the increase in water content, and then tends to remain unchanged. When the maximum axial stress is 16 MPa, 20 MPa, and 24 MPa, the axial strain first increases and then decreases with the increase in the water content, and the curve shows a convex distribution.

When the maximum axial stress is above 16 MPa, the relationship between the strain and water content is very similar to the compaction test. That is, when the water content reaches a certain suitable value, the axial strain of the crushed gangue can reach the maximum value, and with the increase in the stress, the compactness that the crushed gangue can achieve is better.

Following the data processing method of the compaction test, a 4th-order polynomial fitting analysis was performed on the relationship curve between the axial strain and water content when the axial stress was above 16 MPa. The coordinate values of the peak point corresponding to the fitting curve are the optimal water content and maximum axial strain.

Table 3 shows the fitting results of the relationship curve between the axial strain and water content. It can be seen that with the increase in axial stress, the maximum axial strain gradually increases, and the corresponding optimal water content gradually decreases.

Table 3. Fitting results of the relationship between axial strain and water content.

Axial Stress/MPa	Optimal Water Content/%	Maximum Axial Strain
16 MPa	5.11	0.387
20 MPa	4.91	0.398
24 MPa	4.79	0.403

The relationship between the axial strain and water content of crushed gangue is closely related. The moisture in the crushed gangue will affect the frictional resistance and pore structure between the particles. As the water content increases, the lubricating effect of the moisture becomes more obvious, and the corresponding axial strain is relatively larger. At the same time, the moisture in the crushed gangue will fill the pores between the gangue particles, reduce the number and size of the pores, and hinder the further compaction of the gangue particles. Therefore, when the water content reaches a certain level, the axial strain will decrease instead.

3.3. Analysis of the Variation Law of Compression Modulus

The compression modulus is an important characteristic parameter that reflects the deformation resistance of granular materials. Referring to the definition of the compression

modulus of soil, the compression modulus of crushed gangue is simply defined as the slope of the line connecting the point on the axial stress–strain curve with the origin, as shown in Equation (5).

$$E_c = \frac{\sigma_c}{\varepsilon_c} \tag{5}$$

where σ_c, ε_c are the ordinate and abscissa of a point on the stress–strain curve, respectively.

Figure 8 shows the relationship between the compression modulus and the axial stress of the crushed gangue sample. During the confined compaction process, the compression modulus has a linear relationship with the stress, and the compression modulus increases continuously with the increase in the stress.

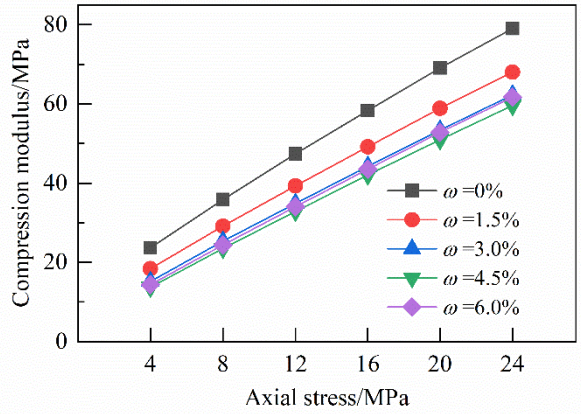


Figure 8. Relationship curves between compression modulus and axial stress.

Table 4 shows the fitting analysis of the compression modulus and axial stress relationship curves under different water contents using a linear function. The linear fitting relationship between the compression modulus and axial stress is good, with R-squared values all above 0.99.

Table 4. Fitting equations for the relationship between compression modulus and axial stress under different water content conditions.

Water Content/%	Fitting Equation	R^2
0	$E_s = 13.5178 + 2.7657\sigma$	0.9988
1.5	$E_s = 9.1559 + 2.4796\sigma$	0.9993
3.0	$E_s = 6.3365 + 2.3501\sigma$	0.9994
4.5	$E_s = 5.0527 + 2.2935\sigma$	0.9996
6.0	$E_s = 5.3232 + 2.3695\sigma$	0.9996

The axial stress and water content are important factors affecting the variation pattern of the compression modulus. It can be seen from Figure 8 that when the axial stress is 4 MPa, the maximum variation in the compression modulus under different water contents is 9.9 MPa. When the axial stress is 24 MPa, the maximum variation in the compression modulus under different water contents is 19.3 MPa. The greater the axial stress, the more obvious the effect of the water content on the compression modulus. Under the same axial stress, the compression modulus of crushed gangue is the largest when the water content is 0, and the variation range is about 23–79 MPa; the compression modulus is the smallest when the water content is 4.5%, and the variation range is about 13.5–60 MPa. With the increase in the water content, the compression modulus shows a trend of first decreasing and then increasing, and the influence of the water content on the compression modulus gradually weakens. This is consistent with the change in the slope of the first-order fitting equation in the table.

3.4. Analysis of Variation Law of Rebound Modulus

The rebound modulus can effectively reflect the ability of crushed gangue to resist axial deformation, and it is closely related to factors, such as the lithology, water content, and compactness. Under confined compaction conditions, the rebound modulus is defined as the ratio of the axial stress to the rebound strain, as shown in Equation (6).

$$E_r = \frac{\sigma}{\varepsilon_r} = \frac{\sigma \cdot h}{h_2 - h_1} \tag{6}$$

where h_1, h_2 represent the height of the crushed gangue sample before and after unloading, respectively.

Figure 9 shows the relationship between the rebound modulus and the axial stress of the confined compaction under different water content conditions of the crushed gangue. Under the action of axial stress, the rebound modulus increases continuously with the increase in the axial stress. When the water content is 1.5% and 3.0%, the change rate of the rebound modulus under axial stress of 4–8 MPa is relatively large. In other cases, the rebound modulus is basically linearly related to stress.

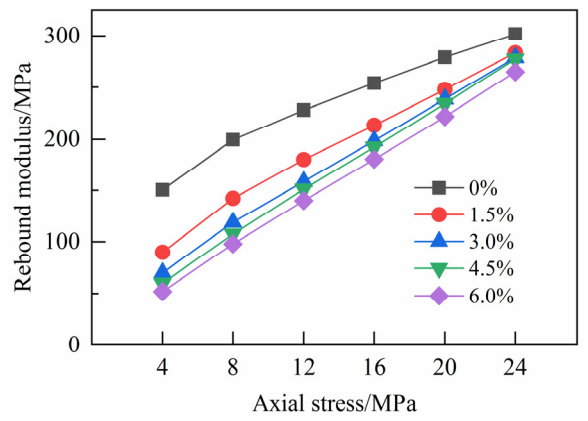


Figure 9. Relation curves of rebound modulus and stress.

When the axial stress is the same, the rebound modulus of crushed gangue decreases gradually with the increase in the water content. This shows that the higher the water content, the smaller the friction between the gangue particles, and the particles are more prone to slip or roll, resulting in a weaker ability of the crushed gangue sample to resist elastic deformation. When the water content of the crushed gangue is 0%, the variation range of the rebound modulus is 151–302 MPa. When the water content of the crushed gangue is 6.0%, the variation range of the rebound modulus is 52–265 MPa. With the increase in axial stress, the influence of the water content on the rebound modulus of crushed gangue gradually decreases.

4. Analysis of the Relationship between Particle Crushing and Compaction Deformation

During the confined compaction process, the gangue particles will continuously move and squeeze, eventually leading to crushing. The factors affecting the crushing of particles are very complex and are related to the lithology, physical and mechanical properties, and gradation of the particles [38]. Through the above series of tests, it was found that the deformation laws of crushed gangue under different water content conditions during compaction are different. This indicates that the particle crushing laws of gangue under different water conditions are also different.

In order to explore the influence of water content on the degree of crushing of crushed gangue samples with the same initial gradation conditions, this study quantified the crushing of gangue particles by calculating the relative crushing rate. Hardin [39] defined the relative crushing rate. Einav [40] further studied and found that particles do not crush

indefinitely as stress increases during compaction. The gradation after crushing eventually tends to a stable state. Therefore, the calculation method for the relative crushing rate was improved, as shown in Equation (7). Figure 10 shows a schematic diagram for calculating the relative crushing rate.

$$B_r = \frac{B_t}{B_p} \tag{7}$$

where B_r is the relative crushing rate; B_t is the crushing amount of gangue, which is the area surrounded by the initial gradation curve and the current gradation curve; and B_p is the crushing potential of gangue, which is the area surrounded by the initial gradation curve and the limit gradation curve area.

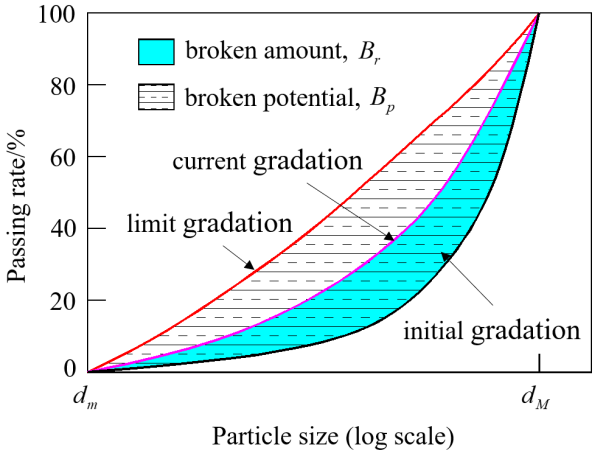


Figure 10. Schematic diagram of calculation of relative crushing rate.

The relative crushing rate of the crushed gangue samples after compaction was calculated according to Equation (7). Figure 11 shows the relationship between the relative crushing rate and axial strain. It can be seen that the relative crushing rate of crushed gangue after compaction increases continuously with the increase in the axial strain, and the increase rate of the relative crushing rate is also gradually increasing. The change law of the relative crushing rate and axial strain is different in dry and water-containing conditions. When the axial strain is the same, the relative crushing rate in the dry conditions is greater than that in the water-containing conditions. The relative crushing rate has a good correlation with axial stress. The data were fitted using a cubic function $B_r = A\varepsilon + B\varepsilon^2 + C\varepsilon^3$, and the R-squared of all the fitting results were above 0.99.

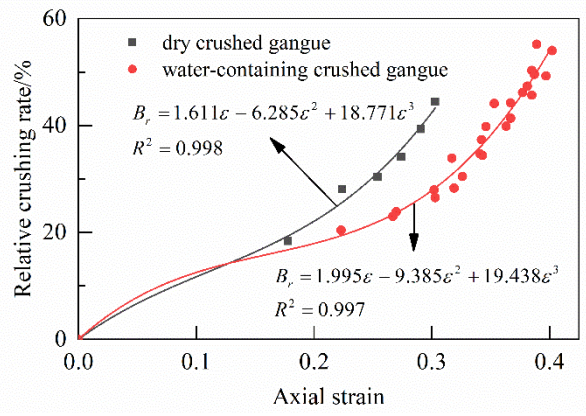


Figure 11. Relationship curves between relative crushing rate and axial strain.

5. Conclusions

Aiming at the problem of the confined compaction deformation of crushed gangue, this paper studied the relationship between the compaction deformation of crushed gangue and the axial stress, water content, and relative crushing rate under different water conditions through confined compaction tests. The main conclusions are as follows:

(1) With the continuous increase in the axial stress, the axial strain of the crushed gangue samples under different water content conditions generally shows a continuous increasing trend, and the curve growth rate gradually decreases. The confined compaction deformation process of crushed gangue can be divided into three stages: the rapid compaction stage, crushing compaction stage, and stable compaction stage. The strain–stress curve will exhibit a serrated shape change at the boundary between the rapid densification stage and the crushing compaction stage.

(2) According to the results of the confined compaction test of crushed gangue, the form of the fitting equation of the strain–stress curve of the confined compaction is modified and improved. Different function forms were used to fit the strain–stress curve for each of the three stages of the confined compaction deformation process. The multi-parameter logarithmic function was still used to fit the strain–stress curve in the rapid densification stage and the crushing compaction stage, while the Chapman–Richards function was used to fit the strain–stress curve in the stable compaction stage. The R-squared of the fitting results were all above 0.99.

(3) The compression modulus of crushed gangue shows a good linear relationship with the water content. The maximum variation in the compression modulus under different water content conditions ranges from 9.9 to 19.3 MPa, and the greater the axial stress, the more obvious the effect of the water content on the compression modulus. When the water content is 1.5% and 3.0%, the variation rate of the rebound modulus under the axial stress of 4–8 MPa is relatively large, while in other cases the rebound modulus shows a basic linear relationship with the axial stress.

(4) There is a good correlation between particle crushing and compaction deformation. The relative crushing rate increases continuously with the increase in the axial strain, and the increase rate of the relative crushing rate also increases gradually. The variation law of the relative crushing rate and axial strain is different in dry conditions and water-containing conditions. When the axial strain is the same, the relative crushing rate in the dry conditions is greater than that in the water-containing conditions.

Author Contributions: Conceptualization, P.L. and Y.Y.; methodology, P.L.; validation, P.L., J.L. and Y.S.; formal analysis, Y.Y.; data curation, P.L.; writing—original draft preparation, C.X.; writing—review and editing, Y.S. All authors have read and agreed to the published version of the manuscript.

Funding: This research was funded by the National Natural Science Foundation of China, grant number 52104088, and also by the Foundation of Liaoning province Department of Education, grant number LJKZ0361.

Institutional Review Board Statement: Not applicable.

Informed Consent Statement: Not applicable.

Data Availability Statement: Not applicable.

Conflicts of Interest: The authors declare no conflict of interest.

References

1. Hu, Z.Q.; Gong, Y.S. *Ecological Restoration of Coal Gangue Dumps*; Science Press: Beijing, China, 2021.
2. Wang, D.M.; Fang, K.Z. *Utilization Technology of Coal Gangue Resource*; China Building Materials Press: Beijing, China, 2021.
3. Gu, L.J.; Shen, Y.J.; Wang, N.Q.; Song, S.J.; Nie, W.J. Pollution characteristics and potential risk assessment of heavy metals in soil of coal gangue accumulation areas. *J. Xi'an Univ. Sci. Technol.* **2022**, *42*, 942–949.
4. Yan, Q.W.; Li, F.; Chao, L.; Dong, J.H. Environmental problems and countermeasures in arid and semi-arid coal mine areas. *Environ. Sustain. Dev.* **2021**, *46*, 79–82.

5. Han, R.C.; Guo, X.N.; Guan, J.F.; Yao, X.H.; Hao, Y. Activation mechanism of coal gangue and its impact on the properties of geopolymers: A review. *Polymers* **2022**, *14*, 3861. [CrossRef]
6. Li, J.Y.; Wang, J.M. Comprehensive utilization and environmental risks of coal gangue: A review. *J. Clean. Prod.* **2019**, *239*, 117946. [CrossRef]
7. Bai, D.S. Ecological Reconstruction Model and Driving Factors of Soil Hydrological Properties Optimization in Gangue Accumulation Area. Ph.D. Thesis, Southwest University of Science and Technology, Mianyang, China, 2022.
8. Li, Z.; Xue, J.; Zhu, Z.L.; Xiong, S.X.; Li, X.Z.; Zhou, A.N.; Liu, L.J.; Yu, W.; Qu, J.Z. Research Progress on Comprehensive Utilization of Coal Gangue. *Conserv. Util. Miner. Resour.* **2021**, *41*, 165–178.
9. Jia, M. The Current situation research on comprehensive utilization of coal gangue. *Conserv. Util. Miner. Resour.* **2019**, *39*, 46–52.
10. Jiang, L.L.; Li, S.F.; Xu, H.W. Research on current situation and treatment countermeasures of ecological restoration of abandoned mines by history. *Nat. Resour. Inf.* **2023**, *1*, 22–27.
11. Wang, Y.T. Status and prospect of harmless disposal and resource comprehensive utilization of solid waste of coal gangue. *Coal Geol. Explor.* **2022**, *50*, 54–66.
12. Chang, J.W.; Du, G.J.; Du, J.L.; Shi, X.L. Current situation of the comprehensive utilization of coal gangue in China and the related problems and recommendations. *China Environ. Prot. Ind.* **2022**, *8*, 13–17.
13. Zhu, L.; Gu, W.Z.; Song, T.Q.; Pan, H.; Liu, Z.C.; Zhang, P.; He, Z.W. Research progress and prospect of coal gangue slurry filling technology in goaf. *Coal Sci. Technol.* **2022**. [CrossRef]
14. Zhao, B.J.; Liu, P.X.; Guo, C.M. Foundation treatment of coal gangue landfills and high fill sites for power plants. *Eng. J. Wuhan Univ.* **2020**, *53*, 245–248.
15. Guo, Z.Z.; Gao, Q.; Li, E.Q.; Lin, C.S. Application of gangue backfilling and reclamation technology in land management of Xuchang coal mine. *Coal Geol. Explor.* **2019**, *47*, 62–64.
16. Liu, J.K.; Li, S.L.; Wang, Z.J.; Zhang, Z.Y.; Huo, X.D. Reinforcement design and application of coal mine transit pool reinforced with coal gangue. *Coal Eng.* **2018**, *50*, 80–83.
17. Di, S.G. Study on the Road Performance of Coal Gangue Subgrade of Highway. Master's Thesis, Chang'an University, Xi'an, China, 2008.
18. Li, L.H.; Long, G.C.; Bai, C.N.; Ma, K.L.; Wang, M.; Zhang, S. Utilization of coal gangue aggregate for railway roadbed construction in practice. *Sustainability* **2020**, *12*, 4583. [CrossRef]
19. Ma, Z.G.; Xiao, J.H.; Wu, Y.L.; Zhang, Q.H. Experimental study on the characteristics of compaction of the saturated broken coal waste. *J. Min. Saf. Eng.* **2004**, *1*, 106–108.
20. Huang, L.T.; Tang, Z.X. Compression test of water immersed coal gangue foundation in mining area. *J. China Coal Soc.* **1996**, *21*, 468–472.
21. Jiang, Z.Q.; Ji, L.J.; Zuo, R.S. Research on mechanism of crushing-compression of coal waste. *J. China Univ. Min. Technol.* **2001**, *30*, 139–142.
22. Wang, W.; Li, H.M.; Xiong, Z.Q.; Su, Y.S.; Zhang, P. Research on the influence of diameter gradation on compressive deformation characteristics of gangues. *Chin. J. Undergr. Space Eng.* **2016**, *12*, 1553–1558.
23. Liu, S.Y.; Tong, L.Y.; Qiu, Y.; Miao, L.C. Crushable effects on engineering mechanical properties of colliery wastes. *Chin. J. Geotech. Eng.* **2005**, *27*, 505–510.
24. Liu, S.Y. Research on the Physical and Mechanical Characteristics of Coal Waste for Dam Building. Master's Thesis, Liaoning Technical University, Fuxin, China, 2007.
25. Liu, N. Research on Compaction Characteristics and Re-Crushing Mechanism of Graded Broken Coal and Rock. Master's Thesis, Xi'an University of Science and Technology, Xi'an, China, 2021.
26. Zheng, K.H.; Du, C.L.; Qiu, B.J. Experimental study on the fractal characteristics of crushing coal and gangue. *J. China Coal Soc.* **2013**, *38*, 1089–1094.
27. Zhang, J.X.; Li, M.; Liu, Z.; Zhou, N. Fractal characteristics of crushed particles of coal gangue under compaction. *Powder Technol.* **2017**, *305*, 12–18. [CrossRef]
28. Rujikiatkamjorn, C.; Indraratna, B.; Chiaro, G. Compaction of coal wash to optimise its utilisation as water-front reclamation fill. *Geomech. Geoengin. Int. J.* **2013**, *8*, 36–45. [CrossRef]
29. Yang, Y.; Wang, B.F.; Zheng, Z.M. Experimental investigation on compaction energy dissipation of coal gangue filling material. *Bull. Chin. Ceram. Soc.* **2016**, *35*, 3511–3516.
30. Wang, Y.M. Study on the Timeliness of Compaction Characteristics of Crushed Gangue. Master's Thesis, China University of Mining and Technology, Xuzhou, China, 2019.
31. Li, B.Y.; Yan, H.; Zhang, J.X.; Zhou, N. Compaction property prediction of mixed gangue backfill materials using hybrid intelligence models: A new approach. *Constr. Build. Mater.* **2020**, *247*, 118633. [CrossRef]
32. Zhang, Z.T. Dynamic Behaviors and the Evolution of Particle Breakage for Coal Gangue Subgrade Filler under Cyclic Loading. Ph.D. Thesis, Hunan University of Science and Technology, Xiangtan, China, 2021.
33. Li, Z.; Fang, Z.L.; Feng, G.R.; Zhao, J.P. Three dimensional acoustic emission location method for crushed coal and rock and its layered fracture characteristics. *J. Taiyuan Univ. Technol.* **2022**, *53*, 507–514.
34. Zhang, T.J.; Wang, X.J.; Pang, M.K.; Zhang, S.; Wang, F. Study on compaction and re-crushing of crushed gangue considering intermittent grading. *J. Cent. South Univ. (Sci. Technol.)* **2023**, *54*, 314–326.

35. Liang, P.F.; Yang, Y.; Huang, H.X.; Liu, J.S.; Guo, N. Experimental study on fractal characteristics of particle size distribution by repeated compaction of road recycling crushed stone. *Appl. Sci.* **2022**, *12*, 10303. [CrossRef]
36. He, Z.Q. Study on Mechanical Behavior of Coal Mine Gangue Filling Material in Compaction Deformation. Master's Thesis, China University of Mining and Technology, Xuzhou, China, 2019.
37. Su, C.D.; Gu, M.; Tang, X.; Guo, W.B. Experiment study of compaction characteristics of crushed stones from coal seam roof. *Chin. J. Rock Mech. Eng.* **2012**, *31*, 18–26.
38. Zhang, C.; Zhao, Y.X.; Tu, S.H.; Hao, X.J.; Hao, D.Y.; Liu, J.B.; Ren, Z.P. Influence mechanism of particle size on the compaction and breakage characteristics of broken coal mass in goaf. *J. China Coal Soc.* **2020**, *45*, 660–670.
39. Hardin, B.O.; Blandford, G.E. Elasticity of particulate materials. *J. Geotech. Eng.* **1989**, *115*, 788–805. [CrossRef]
40. Einav, I. Breakage mechanics–part I: Theory. *J. Mech. Phys. Solids* **2007**, *55*, 1274–1297. [CrossRef]

Disclaimer/Publisher's Note: The statements, opinions and data contained in all publications are solely those of the individual author(s) and contributor(s) and not of MDPI and/or the editor(s). MDPI and/or the editor(s) disclaim responsibility for any injury to people or property resulting from any ideas, methods, instructions or products referred to in the content.